arXiv:2109.11261

THE EFFECT OF ENVIRONMENT ON STAR FORMATION ACTIVITY AND MORPHOLOGY AT $0.5 < Z < 2.5$ IN CANDELS

YIZHOU GU,[1,2] GUANWEN FANG,[3,*] QIRONG YUAN,[1] SHIYING LU,[4] AND SHUANG LIU[1]

ABSTRACT

To explore the effect of environment on star-formation and morphological transformation of high-redshift galaxies, we present a robust estimation of localized galaxy overdensity using a density estimator within the Bayesian probability framework. The maps of environmental overdensity at $0.5 < z < 2.5$ are constructed for the five CANDELS fields. In general, the quiescent fraction increases with overdensity and stellar mass. Stellar mass dominates the star formation quenching for massive galaxies, while environmental quenching tends to be more effective for the low-mass galaxies at $0.5 < z < 1$. For the most massive galaxies ($M_* > 10^{10.8} M_\odot$), the effect of environmental quenching is still significant up to $z \sim 2.5$. No significant environmental dependence is found in the distributions of Sérsic index and effective radius for SFGs and QGs separately. The primary role of environment might be to control the quiescent fraction. And the morphological parameters are primarily connected with star formation status. The similarity in the trends of quiescent fraction and Sérsic index along with stellar mass indicates that morphological transformation is accompanied with star formation quenching.

星形成抑制への環境の影響。

- 銀河はその星形成活動によってSFG/QGに大別され、SFGはdisk-like, QGはspheroidalが多い。
- 星形成の抑制と形態変化の物理過程は複雑で未だ不明なことが多い。
  - Mass quench: haloのhot gasがガス降着を抑制。
  - Morph. quench: 構造が発達してガスが安定化しclumpを形成しない。
  - Environ. quench: ガス剥ぎ取り、ガス降着の抑制。
- CANDELSデータでz~2.5の銀河の星形成・環境・形態を見てみる。
  - QGはUVJ 2色図で選択。
  - ベイズ確率により密度超過を抽出。

従来: $\Sigma_N \propto 1/(\pi d_N^2)$,

↓

$$\Sigma'_N \propto 1/(\Sigma_{i=1}^{N} d_i^2),$$

↓

$$1 + \delta'_N = \frac{\Sigma'_N}{\langle \Sigma'_N \rangle_{\rm uniform}} = \frac{\Sigma'_N}{k'_N \Sigma_{\rm surface}},$$

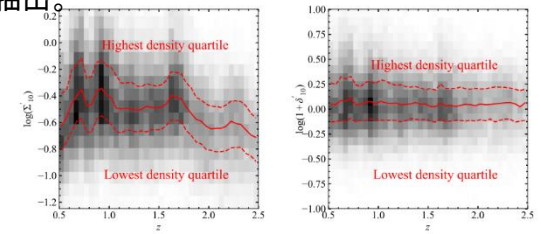

Figure 2. Left: Density indicator Σ'_{10} as a function of redshift. Right: Overdensity $1+\delta'_{10}$ as a function of redshift. T solid and dashed lines are derived by a small redshift interval, $\Delta z = 0.1$, which show the median, bottom, and top quar the distribution. The background represents the distribution of out galaxy sample.

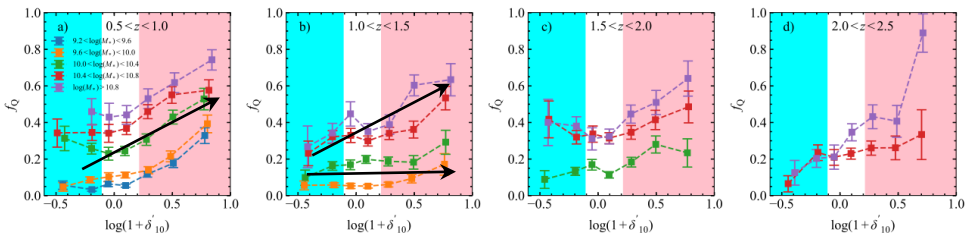

Figure 3. The quiescent fractions change as a function of overdensity at a specified stellar mass range in four redshift bins. The different colors represent galaxies in the different stellar mass bins ($\Delta M_* \sim 0.4$ dex). The pink and cyan regions mark the highest density quartile and the lowest density quartile. The error bars indicate the uncertainties based on Poisson statistics.

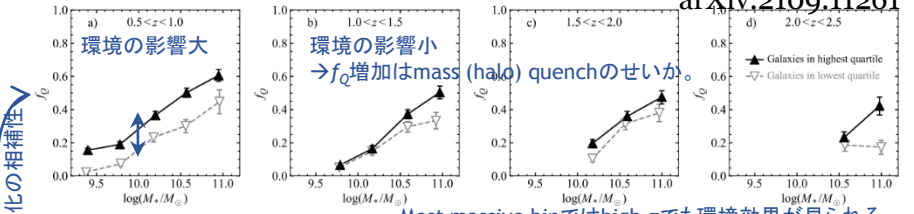

環境の影響大

環境の影響小
→f_Q増加はmass (halo) quenchのせいか。

Most massive binではhigh-zでも環境効果が見られる。

Figure 4. Quiescent fraction as a function of stellar mass at fixed overdensity and redshift bins. The hollow and solid symbols correspond to the lowest density quartile and the highest density quartile. The error bars indicate the uncertainties based on Poisson statistics.

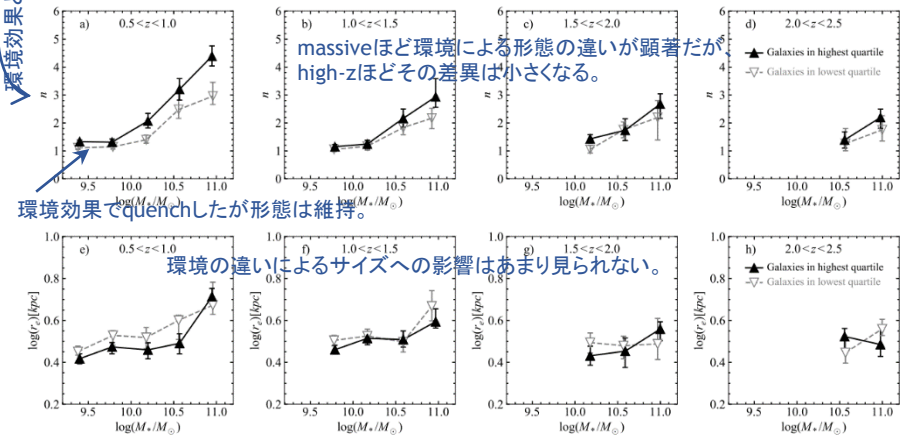

分布が似ている
環境効果と形態進化の相補性

massiveほど環境による形態の違いが顕著だが、high-zほどその差異は小さくなる。

環境効果でquenchしたが形態は維持。

環境の違いによるサイズへの影響はあまり見られない。

Figure 5. Median values of Sérsic indices and effective radii as a function of stellar mass at fixed overdensity and redshift bins. The hollow and solid symbols correspond to the lowest and the highest overdensity quartiles, respectively. The errors are estimated by the bootstrap method with 1000 times resamplings.

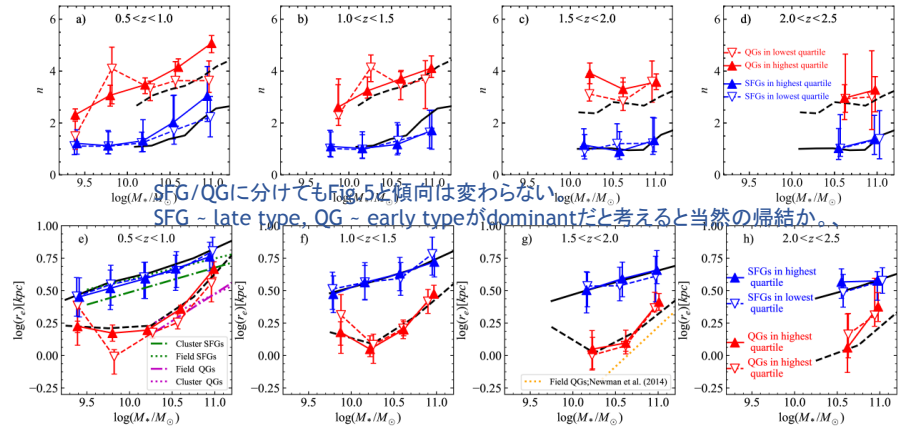

SFG/QGに分けてもFig.5と傾向は変わらない。
SFG ~ late type, QG ~ early typeがdominantだと考えると当然の帰結か。。

Figure 6. Median values of Sérsic indices and effective radii as a function of stellar mass at fixed overdensity and redshift bins. Blue (Solid) and red (dashed) lines represents star-forming galaxies and quiescent galaxies, respectively. Hollow and solid symbols correspond to the lowest density quartile and the highest density quartile. The errors are estimated by the bootstrap method with 1000 times resamplings. On the top panels, the median values of n as a function of stellar mass from Lang et al. (2014) are also presented by black dashed and solid lines, separated by two redshift ranges of $0.5 < z < 1.5$ and $1.5 < z < 2.5$. On the bottom panels, the median values of r_e as a function of stellar mass from van der Wel et al. (2014) are also represented. The size-mass relations from Allen et al. (2016) are denoted by green and magenta lines, and a yellow dot line extracted from Newman et al. (2014).